A Physics-Informed Neural Network Approach for Fault Diagnosis and Protection in Multi-Source Microgrids

Morteza Ghorbani, Farzad Razavi, Ahmad Fakharian*

Department of Electrical Engineering, Qa.C., Islamic Azad University, Qazvin, Iran,
morteza.ghorbanii@iau.ac.ir, farzad.razavi@qiau.ac.ir ahmad.fakharian@iau.ac.ir

Abstract

This study presents a novel Physics-Informed Neural Network (PINN) framework for fault detection and classification in three-phase microgrids. By integrating the physical laws of the power system with simulated voltage and current measurements, the proposed method accurately identifies single-phase, two-phase, and three-phase faults. Evaluation results show that under noise-free conditions, the model achieves an accuracy of 98.1%, precision of 98.1%, recall of 97.8%, and F1-score of 97.9%. Under noisy conditions (signal-to-noise ratio, SNR = 20 dB), it maintains robust performance with an accuracy of 97.0%, precision of 97.0%, recall of 96.8%, and F1-score of 96.9%. Comparative analysis demonstrates that the proposed PINN outperforms conventional machine learning methods, including Support Vector Machine (SVM), k-Nearest Neighbors (KNN), Decision Tree (DT), Random Forest (RF), Artificial Neural Network (ANN), and eXtreme Gradient Boosting (XGBoost), in terms of accuracy, stability, and robustness to noise. These results confirm that the proposed framework provides an efficient and reliable solution for real-time monitoring and protection of multi-source microgrids, enhancing their stability, reliability, and operational safety.

Keywords: Power system protection, AC microgrid, fault detection, fault classification, PNN.
Article history: Received 2025/10/05; Revised 2025/12/02; Accepted 2025/12/12, Article Type: Research paper

https://doi.org/10.82234/IJSEE.2025.1220172

1. Introduction

In recent years, the increasing level of environmental pollution due to the use of fossil fuels has led to a further increase in the use of distributed generation (DG). The use of DGs changes the basis of distribution networks and transforms them from energy delivery systems to active networks [1, 2]. This change, in addition to creating protection problems, has prevented the development of microgrids [3]. Most of the existing fault detection methods generally depend on the magnitude and direction of the fault current, but the integration of electric vehicles and DGs has caused the fault current in microgrids to be bidirectional [4, 5]. For this reason, the importance of studying the protection of AC microgrids has doubled.

Microgrid protection has attracted the attention of many researchers around the world in recent years. Based on the type and application, microgrid protection methods can be divided into two general groups: methods without using telecommunication links and methods based on telecommunication links [6]. In the first category, protection without the need for telecommunications, relays detect faults only by using voltage and current samples of the lines or equipment under protection [7]. Among the methods used in this category are Thevenin equivalent estimation [8], steady-state fault current calculation [9], fault current sequence component analysis [10], empirical mode analysis (EMD) [11] and wavelet analysis [12]. However, the most important weakness of these approaches is the complexity in setting and changing the relay parameters and also the inability to detect changes in the microgrid topology. The combination of wavelet analysis and cross-differential transform has been proposed in [13]. However, these approaches are highly sensitive to noise and transient disturbances caused by switching operations in microgrids. Some other researchers, like [14], have used zero and negative sequence components for

low impedance fault detection and transient components for high impedance faults. Although this method is somewhat effective, it does not fully cover the effect of network transients and topology changes. In [1], a deep learning method optimized with Black Widow is presented for fault detection in microgrids with electric vehicle chargers. Reference [3] presents a combined method of signal processing and deep learning for fault detection. In [15], a high impedance fault detection method in microgrids using the Group Method of Data Handling (GMDH) intelligent model is presented. In [16], active power direction, current amplitude, and instantaneous voltage variations are used to detect low-impedance faults in microgrids equipped with converter-based DG sources. In [17], the phase difference and admittance amplitude at each bus are also used for fault detection. Traveling wave-based methods in [18] enable high-speed fault detection, but they require high sampling rates and complex calculations to determine the wave propagation speed. Reference [19] presents a method based on second-order fuzzy logic for fault detection and classification in power systems. Although this method shows acceptable performance, the fuzzy rules can be difficult to determine. Reference [20] integrates zero-sequence components into the inverse-time characteristics of phase overcurrent relays (OCRs) and establishes a dynamic scheme between two group settings for phase and ground faults. Reference [21] proposes an improved distance protection scheme with an artificial neural network (ANN) to improve the accuracy of fault detection, classification, and localization in DER-rich microgrids. Although this method shows good performance, it still suffers from the problem of not considering the microgrid controller. Reference [22] employs a combination of traveling waves (TW) and a physics-informed machine learning approach for fault detection and localization in DC microgrids. One of the main limitations of this work is the lack of modeling for various distributed energy resources and storage units. Reference [23] provides a comprehensive review of Physics-Informed Neural Networks in the context of grid-connected inverters. Reference [24] presents a hybrid optimization approach for enhancing the DC-link voltage stability in photovoltaic and wind-based microgrids, addressing the challenges arising from the intermittent nature of renewable energy sources. Reference [25] utilizes a method based on the integration of deep learning and machine learning models for fault detection and localization in DC microgrids. The major drawback of this method is its high sensitivity to signal noise.

In the second group, namely telecommunications-based protection, changes in the microgrid operating conditions or in its topology structure are detected by a central protection unit (CPU). This unit constantly monitors the network and updates the relay settings in case of changes. This type of protection is called adaptive protection. Since a large part of microgrid protection methods are adaptive, extensive research has been conducted in this area. In [26], offline adaptive methods are introduced in which all possible settings related to the microgrid structural uncertainties are stored. However, these approaches are not practical due to the need for very large storage space and the inability to cover all changes in the microgrid topology. To solve this problem, in [27 and 28], it has been proposed to re-run the protection coordination calculations after each change in the microgrid .Also in [29], a two-stage adaptive protection method is presented: in the first stage, the fault is detected by conventional methods; if the detection is correct, the system returns to normal; otherwise, the second stage is activated, and the protection coordination calculations are performed, and the relay settings are changed. This method is not practical in large networks because it requires a large amount of computation. Reference [30] introduces an end-to-end protection framework that provides real-time system monitoring, fault-related decision-making, and circuit breaker control. This is achieved by designing distributed data-driven techniques based on the support vector machine method, in which each relay is responsible for distributed data collection, fault detection, fault localization, and fault isolation. Local communication is established between neighboring relays, enhancing cooperative fault localization and isolation. Reference [31] presents an adaptive hybrid trip-based protection strategy for microgrids that enables fast and reliable response to faults using phase voltage and current measurements from relay locations. The protection coordination problem was addressed by optimizing relay settings for different microgrid operational scenarios, which ensures proper coordination between primary and backup relays.

As mentioned, in recent years, the development and operation of three-phase microgrids as one of the key pillars of smart grids has received special attention. By combining distributed generation resources including photovoltaic (PV) units, wind turbines, diesel generators (DG) and energy storage systems (batteries), microgrids provide the possibility of increasing the efficiency, flexibility and resilience of power grids. However, the dynamic and decentralized nature of these networks creates new challenges in the field of protection and monitoring. Topology changes, the occurrence of transient faults, classical protection methods, and even conventional data-driven algorithms may not

perform reliably in the presence of renewable resources with nonlinear and variable behavior. These methods usually require a large volume of labeled data, are sensitive to noise and do not have sufficient generalization ability in unknown operating conditions. Hence, the development of intelligent frameworks that utilize both simulated data and the physical laws of the power system has become a research and industrial necessity.

For this reason, in this paper, a novel framework based on Physics-Informed Neural Networks (PINN) is presented for the protection and monitoring of three-phase microgrids. The microgrid model, including PV sources, a wind turbine, DG and a battery, which were simulated in Simulink/Matlab environment, and voltage and current data were extracted from different points of the network. Then, the data is transferred to the Google Colab environment, and the proposed PINN algorithm is implemented in the Python platform. In addition to detecting the occurrence of the fault, the proposed approach is also able to correctly classify the type of fault. The classification includes types of single-phase to ground faults (AG, BG, CG), two-phase (AB, AC, BC), three-phase (ABC) and fault-free state. Unlike conventional machine learning methods that rely solely on empirical data, PINN reduces the need for extensive training data by incorporating the physical equations governing the power system into the cost function and increases the generalizability of the model to different operating scenarios. This makes the model more robust to noise and has reliable prediction capabilities even in situations where no data has been seen for them. Simulation results show that the developed framework is able to detect faults with high accuracy and correctly identify their type in real time, which improves protection performance and increases the stability and reliability of the microgrid.

The structure of the paper is organized as follows: In the second section, a review of the theoretical foundations and concepts related to physically informed neural networks is presented. In the third section, the simulated microgrid model and simulation results are presented. In the fourth section, a comparison between the proposed method and existing intelligent methods is presented.

2. Formulation

In this paper, the aim is to present a novel PINN-based method for modeling and protecting microgrids including distributed generation resources such as photovoltaic (PV) systems, battery energy storage systems (BESS) and wind turbines. Due to their nonlinear nature, complex dynamics and the behavior dependent on environmental conditions, these resources pose numerous challenges for their accurate modeling and intelligent protection. The use of PINNs, by combining measured data and physical knowledge of the system, allows for training models with high accuracy and generalizability that cannot be achieved in traditional data-only methods.

A) Microgrid Resource Modeling

In the first part, we discussed the DG physical modeling of the generator type. Distributed generators are among the key resources whose voltage and current control is crucial for maintaining grid stability. The dynamic equations of DG voltage and current can be presented using equations (1) and (2).

$$\frac{dV_{DG}(t)}{dt} = \frac{1}{V^T}\left(V_{DG}(t) - V_{ref}\right) + \Delta V_{fault}(t) \quad (1)$$

$$\frac{dI_{DG}(t)}{dt} = \frac{1}{I^T}\left(I_{DG}(t) - I_{ref}\right) + \Delta I_{fault}(t) \quad (2)$$

Where, $V_{DG}(t)$ and $I_{DG}(t)$ are the DG output voltage and current; V^T and I^T are the reference values set by the controller; V^T and I^T are the time constants of the voltage and current response, and $\Delta V_{fault}(t)$ and $\Delta I_{fault}(t)$ are the effects of possible errors on voltage and current.

In the second section, we discussed the modeling of the Photovoltaic (PV). The voltage and current output of the solar panel are nonlinear and depend on the intensity of solar radiation and temperature. Accordingly, the PV model can be expressed based on equations (3) and (4).

$$V_{PV}(t) = \Delta V_{fault}^{PV}(t) + \eta_{PV}.G(t).V_{nom}.sin(2\pi ft) \quad (3)$$

$$I_{PV}(t) = \Delta I_{fault}^{PV}(t) + \frac{P_{PV}(t)}{V_{PV}(t)} \quad (4)$$

Where, η_{PV} is the panel efficiency, $G(t)$ the solar radiation intensity at time *t*, V_{nom} the nominal voltage, and $\Delta V_{fault}^{PV}(t)$ and $\Delta I_{fault}^{PV}(t)$ are the variations due to the error.

Equations (5) - (7) can be used to model a wind turbine.

$$P_{wind}(t) = \frac{1}{2}\rho A C_P V_{wind}^3(t) \quad (5)$$

$$V_{wind}(t) = k_{wind}P_{wind}(t)\,sin(2\pi ft) + \Delta V_{fault}^{wind}(t) \quad (6)$$

$$I_{wind}(t) = \frac{P_{wind}(t)}{V_{wind}(t)} + \Delta I_{fault}^{wind}(t) \quad (7)$$

Batteries are modeled as energy storage sources, considering the dynamic charging and discharging presented in equation (8).

$$\frac{dSoc}{dt} = \frac{P_{bat}(t)}{C_{bat}} \quad (8)$$

The battery output voltage and current can be calculated from equations (9) and (10).

$$V_{bat}(t) = V_{nom}Soc(t)\,sin(2\pi ft) + \Delta V_{fault}^{bat}(t) \quad (9)$$

$$I_{bat}(t) = \frac{P_{bat}(t)}{V_{bat}(t)} + \Delta I_{fault}^{bat}(t) \quad (10)$$

B) PINN Framework for Fault Detection and Classification

The PINN network receives inputs including time, environmental parameters (irradiance intensity, wind speed, battery SoC), and initial voltage and current data of the resources; its output is the voltage and current prediction as well as the fault class label based on equations (11) and (12).

$$X = [t, G(t), V_{wind}(t), Soc(t), \dots] \quad (11)$$

$$y' = [V'_{DG}, I'_{DG}, V'_{PV}, I'_{PV}, V'_{wind}, I'_{wind}, V'_{bat}, I'_{bat}, \hat{y}_{fault}] \quad (12)$$

The cost function can be defined as equation (13):

$$\zeta = \underbrace{\zeta_{data}}_{\text{math data}} + \lambda_1 \underbrace{\zeta_{physics}}_{\text{physics constraints}} + \lambda_2 \underbrace{\zeta_{fault\ classification}}_{\text{fault class}} \quad (13)$$

Where ζ_{data}, $\zeta_{physics}$, and $\zeta_{fault\ classification}$ can be calculated from equations (14) to (16).

$$\zeta_{data} = \frac{1}{N}\sum_{i=1}^{N}\sum_{s}(\|V'_s(t_i) - V_s^{mean}(t_i)\|^2 + \|I'_s(t_i) - I_s^{mean}(t_i)\|^2) \quad (14)$$

$$\zeta_{physics} = \frac{1}{N}\sum_{i=1}^{N}\sum_{s}\left(\|N_{v,s}(V_s, t_i)\|^2 + \|N_{i,s}(I_s, t_i)\|^2\right) \quad (15)$$

$$\zeta_{fault\ classification} = -\frac{1}{N}\sum_{i=1}^{N}\sum_{c=1}^{C} y_{i,c}\, log(y'_{i,c}) \quad (16)$$

Here, $N_{v,s}$ and $N_{i,s}$ represent the differential equations for each source. To train the PINN model, 4000 data samples were generated, including error and non-error conditions. The model inputs include time, solar radiation, wind speed, battery state of charge (SoC), storage mode voltage and current, while the outputs include error labels. The network architecture consists of three hidden layers with 128 neurons and a tanh activation function. Optimization was performed using the Adam algorithm with a learning rate of 0.001, batch size 64 and 2000 training sessions. The overall cost function consists of three parts: data error, physical error and classification error. The model performance is evaluated using the confusion matrix. The PINN model settings are presented in Table (1). Figure (1) shows the proposed fault detection algorithm based on the PINN model.

3. Simulation Results

A) The Studied Network

To investigate the method presented in this paper, the standard CIGREE network has been used, which includes PV, WIND, synchronous generator and storage. This network is shown in Figure (2) [32]. This system consists of an 11-node system connected to the main network through a transformer. The network operates at a voltage of 20 kV and a frequency of 50 Hz. The switches S1, S2 and S3 are responsible for changing the operating mode of the network (it is assumed that the switch S1 is closed and the switches S2 and S3 are open) [32]. The addition of a battery storage system and a synchronous generator is a minor modification to the original model. The distances are maintained, and the relevant parameters are adjusted accordingly. The overhead line parameters are estimated with the π model and hyperbolic corrections. For the balanced three-phase transmission line model, the parameters are integrated. The parameters R, L and C are positive and include zero sequence parameters to account for inductive and capacitive couplings between the three-phase conductors. The RLC parameters used in the simulations are as follows:

- *R0 = 0.6581 ohm/km*
- *R1 = 0.5132 ohm/km*
- *L0 = 0.0051 H/km*
- *L1 = 0.0012 H/km*
- *C0 = 4.0744 nF/km*
- *C1 = 10.0971 nF/km*

Table (2) shows the branches of the system along with the length of overhead lines and the power of the loads connected to each node. Nodes that do not have loads are marked with "–".

Table.1.
PINN model parameter settings

Parameter	*Value*
Number of training data	4000
Data ratio	70% training, 30% testing
Inputs	Time tt, Solar radiation GG, Wind speed, SoC, Storage status, Voltage and current
Outputs	Error label
Network structure	Dense layers with 128 neurons
Activation function	tanh
Outputs (Heads)	3 voltage neurons, 3 current neurons, 2 classification neurons (Softmax)
Optimizer	Adam
Learning rate	0.001
Batch size	64
Number of training sessions	2000
Cost function components	Data Loss + Physics Loss + Classification Loss
Evaluation criteria	Confusion Matrix

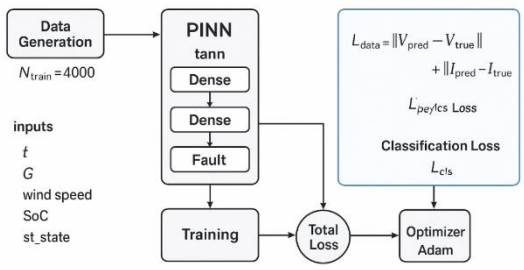

Fig. 1. Algorithm of the proposed PINN method

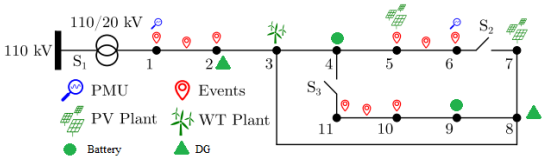

Fig. 2. The network under study [32].

Table.2.
Length of overhead lines, branches and the power of the connected loads [32].

Node From	*Node To*	*Length (km)*	*Load Power (kVA)*
1	2	2.82	20400
2	3	4.42	–
3	4	0.61	560
3	8	1.30	–
4	5	0.56	445
4	11	0.49	–
5	6	1.54	750
6	7	0.24	565
7	8	1.67	90
8	9	0.32	605
9	10	0.77	675
10	11	0.33	570

All datasets used for training and evaluating the proposed PINN model were obtained from time-domain simulations conducted in the MATLAB/Simulink environment. After defining the operating conditions and fault scenarios, the instantaneous three-phase voltage and current signals were recorded at several measurement nodes within the microgrid. These measurements capture both the steady-state behavior of the system and the transient signatures associated with different types of faults. To ensure accurate representation of fast dynamic events, all signals were sampled at a frequency of 20 kHz. Each simulation run covered a duration of 0.1 seconds, providing a uniform time window across all cases. The recorded data include the three-phase voltage and current waveforms at each measurement point. A wide range of scenarios was simulated to create a diverse and representative dataset. These scenarios include normal (fault-free) operation, single-phase-to-ground faults (AG, BG, CG), line-to-line faults (AB, AC, BC), and three-phase faults (ABC). Different fault locations and fault impedances were also considered to introduce variability and improve the generalization capability of the model. In addition, the dataset reflects different operating conditions of the distributed energy resources to ensure that the model remains robust under varying system states.

Figure 3 shows the Simulink implementation of the PV, wind turbine, DG, and BESS components. After completing the simulations, the data were exported to CSV files, which were subsequently imported into the Python environment in Google Colab. These files served as the input for training and evaluating the proposed Physics-Informed Neural Network (PINN) framework. This workflow enables a clear and efficient integration between MATLAB/Simulink and Python, combining realistic microgrid simulations with advanced machine learning-based fault diagnosis.

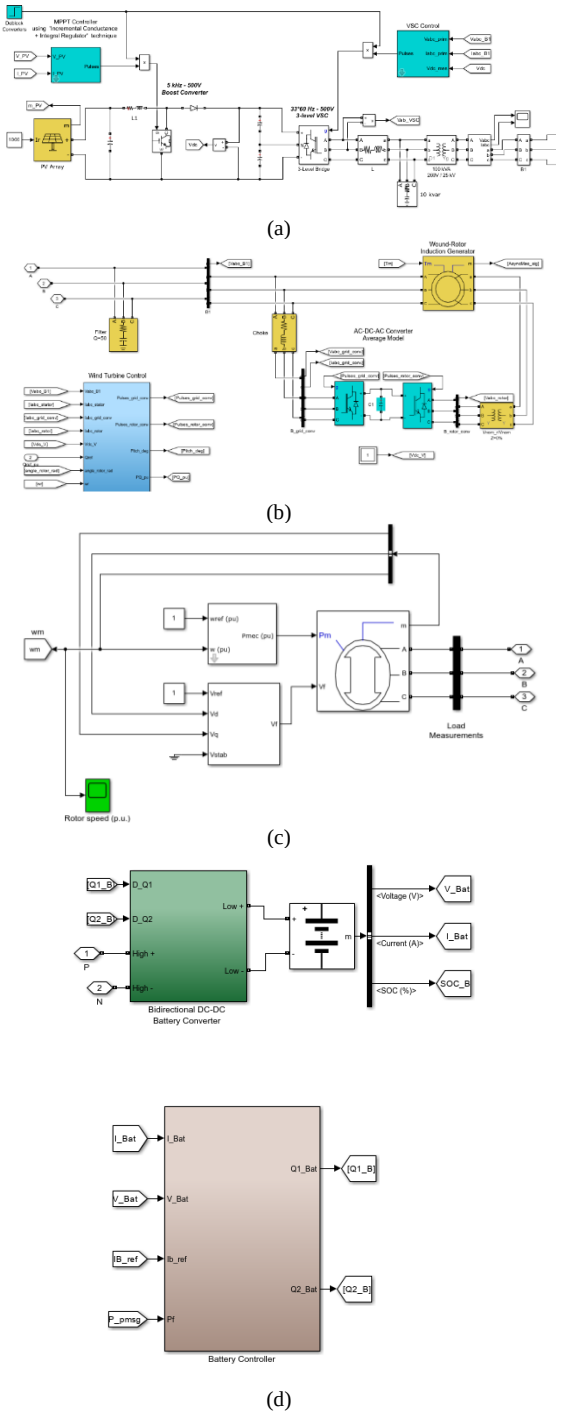

Fig. 3. Simulink implementation of distributed energy resources in the microgrid: (a) PV unit, (b) WT, (c) DG, and (d) BESS.

B) Case 1: Noiseless Network

The results of identifying and classifying error types in the noiseless state are shown in Table 3 and

also in Figure 4 (confusion matrix). According to this table, the proposed PINN-based method has been able to provide very accurate performance in all error and normal states, such that the Precision, Recall and F1-score values are all higher than 0.97. This indicates the high power of the method in correctly separating different classes and reducing type I and type II errors.

In particular, for single-phase faults such as AG and BG, the F1-score values are 0.979 and 0.980, respectively, indicating a very accurate identification of these states. Also, for two-phase faults (such as AB, AC, and BC) and three-phase faults (ABC), the F1-score values are 0.979, 0.987, 0.983, and 0.985, respectively, indicating the same and balanced performance of the model in all states. On the other hand, in the no-fault state, the proposed algorithm with an F1-score of 0.987 was able to correctly identify the healthy conditions of the network. Overall, the results of this section show that in noise-free conditions, the proposed method has an accuracy of close to 100% in identifying and classifying various network faults.

C) Case 2: Noisy network

The performance of the proposed method in the presence of noise with different SNR values is shown in Table (4) and also in Figures (5 to 7) (corresponding confusion matrices). The results indicate that the PINN-based model is able to accurately identify errors and the normal state of the network even in noisy conditions. In the case of 60 dB noise, the values of the evaluation indices remain almost the same as in the case of no noise, so that the overall accuracy of the model is reported to be 0.981. This shows that the proposed method is very robust to low-level noise, and there is no noticeable change in its performance.

By reducing the signal-to-noise ratio to 40 dB, the F1-score values are still maintained above 0.97 in most cases, and the overall accuracy is 0.977. These results show that the model has a high ability to classify faults even in moderate noise conditions, and its performance degradation is very limited. In more severe conditions, i.e. 20 dB, although some decrease in accuracy is evident, the F1-score indices still remain above 0.96, and the overall accuracy is 0.970.

These results indicate the stability of the proposed method against severe noise and its ability to correctly identify different network states. In general, comparing the results of three different noise levels shows that the proposed method has a stable and accurate performance not only in the noise-free state, but also in noisy conditions and can be used as an efficient tool for monitoring and protecting power systems.

Table.3.
Fault classification results in noise-free mode

Fault type	***Precision***	***Recall***	***F1-score***
AG	0.978	0.980	0.979
BG	0.974	0.986	0.980
CG	0.986	0.982	0.984
AB	0.982	0.976	0.979
AC	0.992	0.982	0.987
BC	0.984	0.982	0.983
ABC	0.982	0.988	0.985
No fault	0.986	0.988	0.987

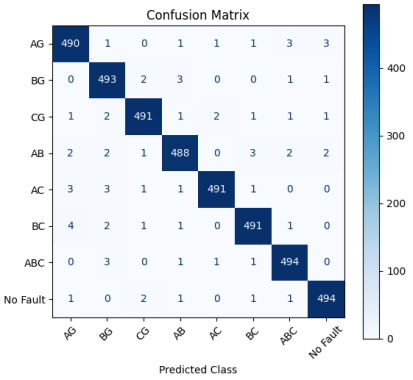

Fig. 4. Confusion matrix from the noise-free test

Table.4.
Fault classification results in noisy conditions (SNR = 60, 40, and 20 dB)

Fault Type	***Precision***	***Recall***	***F1-score***	***Precision***	***Recall***	***F1-score***	***Precision***	***Recall***	***F1-score***
		60 dB			**40 dB**			**20 dB**	
AG	0.986	0.988	0.987	0.982	0.968	0.975	0.955	0.966	0.960
BG	0.972	0.980	0.976	0.982	0.98	0.984	0.970	0.968	0.969
CG	0.982	0.990	0.986	0.974	0.980	0.977	0.968	0.972	0.970
AB	0.986	0.984	0.985	0.972	0.988	0.980	0.986	0.966	0.976
AC	0.980	0.978	0.979	0.974	0.978	0.976	0.978	0.972	0.975
BC	0.982	0.968	0.975	0.978	0.968	0.973	0.968	0.970	0.969
ABC	0.972	0.982	0.977	0.980	0.978	0.979	0.970	0.976	0.973
No Fault	0.988	0.978	0.983	0.974	0.970	0.972	0.966	0.970	0.968
Total accuracy		**0.981**			**0.977**			**0.970**	

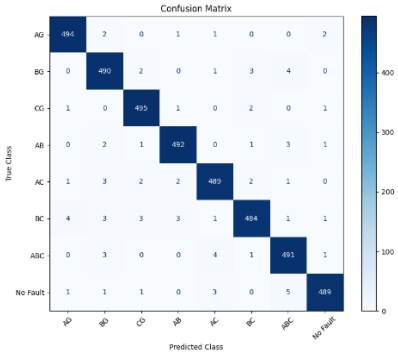

Fig. 5. Confusion matrix resulting from the 60 dB noise mode

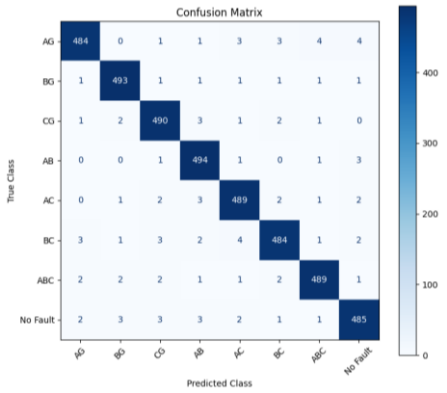

Fig. 6. Confusion matrix resulting from the 40 dB noise mode

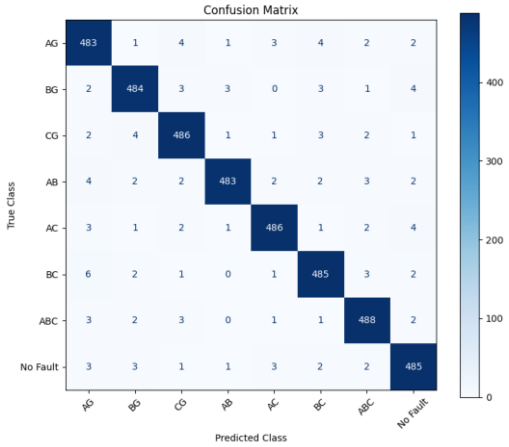

Fig. 7. Confusion matrix from the 20 dB noise test case

D) Case 3: Simultaneous Faults

In order to evaluate the model's ability to cope with more complex conditions, a scenario of the simultaneous occurrence of multiple faults in a microgrid was investigated. In this case, faults were applied simultaneously on lines 3–8 and 10–9, as well as on lines 4–5 with switch S3 closed. For each combination, single-phase, two-phase and three-phase faults (AG, BG, CG, AB, AC, BC, ABC) were applied, and the proposed model was able to correctly identify the fault occurrence and accurately classify the fault type in all scenarios. The results of this investigation are presented in Table (5). This result shows that the PINN-based framework has stable and reliable performance in multiple fault conditions in addition to simple scenarios and can be used as an effective protection solution in operational microgrids.

E) Case 4: Transients

One of the important criteria in the design of protection systems is the ability to distinguish between real faults and transient phenomena that should not lead to relay operation. For this purpose, in this scenario, several transient states were examined, including load connection and disconnection, sudden changes in the generated power of DG and PV sources, topology changes with the opening and closing of switches, as well as transient voltage drops and increases (sag/swell). The results of this analysis are presented in Table (6). The results showed that the proposed model did not recognize any of these transient phenomena as faults, and the false trip rate was equal to zero. This confirms the high accuracy and reliability of the proposed framework under variable operating conditions of the microgrid.

Table.5.
Results when applying multiple simultaneous faults

Faults	***Fault location***	***Fault Type***	***Model Detection***	***Model Classification***
Simultaneous fault 1	Line 3–8 and Line 10–9	AG	Correct	Correct
Simultaneous fault 2	Line 3–8 and Line 10–9	BG	Correct	Correct
Simultaneous fault 3	Line 3–8 and Line 10–9	CG	Correct	Correct
Simultaneous fault 4	Line 3–8 and Line 10–9	AB	Correct	Correct
Simultaneous fault 5	Line 3–8 and Line 10–9	AC	Correct	Correct
Simultaneous fault 6	Line 3–8 and Line 10–9	BC	Correct	Correct
Simultaneous fault 7	Line 3–8 and Line 10–9	ABC	Correct	Correct
Simultaneous fault 8	Line 4–5 (S3 closed)	AG	Correct	Correct
Simultaneous fault 9	Line 4–5 (S3 closed)	BG	Correct	Correct
Simultaneous fault 10	Line 4–5 (S3 closed)	CG	Correct	Correct
Simultaneous fault 11	Line 4–5 (S3 closed)	AB	Correct	Correct
Simultaneous fault 12	Line 4–5 (S3 closed)	AC	Correct	Correct
Simultaneous fault 13	Line 4–5 (S3 closed)	BC	Correct	Correct
Simultaneous fault 14	Line 4–5 (S3 closed)	ABC	Correct	Correct

Table.6.
Results when applying transient states to the network

Test No.	***Transient type***	***Location***	***Fault detection***
1	Sudden load connection	Bus 4	No fault
2	Sudden load disconnection	Bus 6	No fault
3	Sudden DG power change	Near Bus 2	No fault
4	PV output power change (radiation reduction)	Bus 7	No fault
5	S3 switch opening	Line 4–5	No fault
6	S3 switch closing	Line 4–5	No fault
7	Transient voltage drops (Voltage Sag)	Main Bus	No fault
8	Transient voltage increase (Voltage Swell)	Main Bus	No fault

4. Comparison

To comprehensively evaluate the performance of the proposed method, its results under both

noiseless and noisy conditions (SNR = 40 dB) were compared with several common machine learning algorithms, including Support Vector Machine (SVM), k-Nearest Neighbors (KNN), Decision Tree (DT), Random Forest (RF), Artificial Neural Network (ANN), and eXtreme Gradient Boosting (XGBoost). All comparative methods were fully implemented by the authors using the same dataset as the proposed PINN method, ensuring a fair and reliable evaluation.

The results of this comparison are presented in Table 7. In the noiseless condition, the proposed PINN-based method achieved an overall accuracy of 0.985, outperforming all other algorithms. Its closest competitors were ANN (accuracy 0.971), RF (0.965), and XGBoost (0.974). Under noisy conditions (SNR = 40 dB), the PINN method still provided the best performance with an overall accuracy of 0.977, followed by ANN (0.958), RF (0.950), and XGBoost (0.960), while SVM, KNN, and DT showed a notable decrease in performance. These results indicate that the proposed PINN method is the most stable and accurate approach, demonstrating significant robustness and superiority over classical machine learning algorithms in both ideal and noisy environments.

Table.7.
Comparison of the performance of the proposed method with other machine learning methods in noise-free and noisy conditions (SNR = 40 dB)

Method	*Precision (No Noise)*	*Recall (No Noise)*	*F1-score (No Noise)*	*Accuracy (No Noise)*	*Precision (40 dB)*	*Recall (40 dB)*	*F1-score (40 dB)*	*Accuracy (40 dB)*
PINN	0.985	0.984	0.985	0.985	0.978	0.976	0.977	0.977
SVM	0.962	0.960	0.961	0.961	0.950	0.944	0.947	0.945
KNN	0.948	0.944	0.946	0.945	0.938	0.932	0.935	0.933
DT	0.936	0.930	0.933	0.932	0.922	0.918	0.920	0.919
RF	0.968	0.964	0.966	0.965	0.957	0.950	0.953	0.952
ANN	0.972	0.970	0.971	0.971	0.962	0.956	0.959	0.958
XGBoost	0.975	0.973	0.974	0.974	0.964	0.958	0.961	0.960

5. Conclusion

In this paper, a novel framework based on Physics-Informed Neural Networks (PINN) was developed for fault detection and classification in three-phase microgrids. Unlike conventional methods that rely solely on experimental or simulation data, the proposed approach effectively integrates physical knowledge of the power system with numerical measurements, enabling improved performance under practical operating conditions. Simulation results demonstrate that the proposed PINN model can accurately identify all types of fault states as well as normal operating conditions, achieving nearly 99% accuracy in noise-free scenarios. In the presence of measurement noise, the method maintains stable and reliable performance, with overall accuracy exceeding 97% even under challenging conditions (SNR = 20 dB). Comparative analysis with other machine learning algorithms, including SVM, KNN, DT, RF, ANN, and XGBoost, shows that the proposed method consistently outperforms these approaches in terms of precision, recall, F1-score, and overall accuracy, both in noise-free and noisy conditions. This highlights the capability of PINN to learn complex network dynamics while remaining robust to noise. Overall, the results confirm that the proposed PINN-based framework is a reliable and efficient solution for real-time protection and monitoring of multi-source microgrids. Its application can significantly enhance the reliability, safety, and sustainability of future power systems, providing a practical tool for smart grid operations.

References

[1] S. A. Hosseini, B. Taheri, S. H. H. Sadeghi, and A. Nasiri, "A deep learning model for fault detection in distribution networks with high penetration of electric vehicle chargers," e-Prime-Advances in Electrical Engineering, Electronics and Energy, vol. 10, p. 100845, 2024.

[2] Y. Li, B. Feng, B. Wang, and S. Sun, "Joint planning of distributed generations and energy storage in active distribution networks: A Bi-Level programming approach," Energy, vol. 245, p. 123226, 2022.

[3] B. Taheri, S. A. Hosseini, and H. Hashemi-Dezaki, "Enhanced fault detection and classification in ac microgrids through a combination of data processing techniques and deep neural networks," Sustainability, vol. 17, no. 4, p. 1514, 2025.

[4] R. Pradhan and P. Jena, "An innovative fault direction estimation technique for AC microgrid," Electric Power Systems Research, vol. 215, p. 108997, 2023.

[5] S. F. Zarei and S. Khankalantary, "Protection of active distribution networks with conventional and inverter-based distributed generators," International Journal of Electrical Power & Energy Systems, vol. 129, p. 106746, 2021.

[6] H. Jahanbani, F. Razavi, and H. Nafisi, "Presenting an innovative single-setting adaptive protection method for AC microgrid with wind turbine," Electrical Engineering, pp. 1-16, 2024.

[7] M. Ghotbi-Maleki, R. M. Chabanloo, H. H. Zeineldin, and S. M. H. Miangafsheh, "Design of setting group-based overcurrent protection scheme for active distribution networks using MILP," IEEE Transactions on Smart Grid, vol. 12, no. 2, pp. 1185-1193, 2020.

[8] S. Shen et al., "An adaptive protection scheme for distribution systems with DGs based on optimized Thevenin equivalent parameters estimation," IEEE Transactions on Power Delivery, vol. 32, no. 1, pp. 411-419, 2015.

[9] J. Ma, X. Wang, Y. Zhang, Q. Yang, and A. Phadke, "A novel adaptive current protection scheme for distribution systems with distributed generation," International Journal of Electrical Power & Energy Systems, vol. 43, no. 1, pp. 1460-1466, 2012.

[10] H. Muda and P. Jena, "Superimposed adaptive sequence current based microgrid protection: A new technique," IEEE Transactions on Power Delivery, vol. 32, no. 2, pp. 757-767, 2016.

[11] B. Taheri and A. Shahhoseini, "Direct current (DC) microgrid control in the presence of electrical vehicle/photovoltaic (EV/PV) systems and hybrid energy storage systems: A Case study of grounding and protection issue," IET Generation, Transmission & Distribution, vol. 17, no. 13, pp. 3084-3099, 2023.

[12] R. Eslami and S. A. Hosseini, "A comprehensive method for fault detection in AC/DC hybrid microgrid," Electric Power Components and Systems, vol. 50, no. 1-2, pp. 38-51, 2022.

[13] H. Huang, Z. Gong, H. Shu, and X. Tian, "Microgrid fault detection method based on sequential overlapping differential transform," in 2020 IEEE 4th Conference on Energy Internet and Energy System Integration (EI2), 2020: IEEE, pp. 2308-2313 .

[14] M. A. Zamani, T. S. Sidhu, and A. Yazdani, "A protection strategy and microprocessor-based relay for low-voltage microgrids," IEEE transactions on Power Delivery, vol. 26, no. 3, pp. 1873-1883, 2011.

[15] B. Taheri, S. A. Hosseini, S. Salehimehr, and F. Razavi, "A novel approach for detection high impedance fault in DC microgrid," in 2019 International Power System Conference (PSC), 2019: IEEE, pp. 287-292 .

[16] J. O. C. P. Pinto and M. Moreto, "Protection strategy for fault detection in inverter-dominated low voltage AC microgrid," Electric Power Systems Research, vol. 190, p. 106572, 2021.

[17] F. Zhang and L. Mu, "New protection scheme for internal fault of multi-microgrid," Protection and Control of Modern Power Systems, vol. 4, no. 2, pp. 1-12, 2019.

[18] X. Dong and S. Shi, "Identifying single-phase-to-ground fault feeder in neutral noneffectively grounded distribution system using wavelet transform," IEEE Transactions on Power Delivery, vol. 23, no. 4, pp. 1829-1837, 2008.

[19] D. Mlakić, S. Nikolovski, and H. R. Baghaee, "Cyber–physical machine-learning-based grid-fault detection and location scheme for distance protection of MV distribution lines," International Journal of Electrical Power & Energy Systems, vol. 171, p. 111029, 2025.

[20] Ghanem et al., "Advanced microgrid protection utilizing zero sequence components with Hard-Ware-in-the-Loop testing," IEEE Access, 2025.

[21] Sheta, A. A. Eladl, B. E. Sedhom, M. I. El-Afifi, P. Sanjeevikumar, and M. Zaki, "Artificial neural network-based enhanced distance protection sensitivity in microgrids," Renewable Energy Focus, vol. 54, p. 100710, 2025.

[22] Paruthiyil, Sajay Krishnan, Ali Bidram, and Matthew J. Reno. "A physics-informed learning technique for fault location of DC microgrids using traveling waves." IET Generation, Transmission & Distribution 16.23 (2022): 4791-4805.

[23] Mahdouri, Ekram Al, et al. "Physics-Informed Neural Networks in Grid-Connected Inverters: A Review." Energies 18.20 (2025): 5441.

[24] Tanuja, H. "Enhancing voltage stability in photovoltaic and wind micro grids with a hybrid optimization approach." Computers and Electrical Engineering 123 (2025): 110025.

[25] Salehimehr, Sirus, Seyed Mahdi Miraftabzadeh, and Morris Brenna. "A novel machine learning-based approach for fault detection and location in low-voltage dc microgrids." Sustainability 16.7 (2024): 2821.

[26] P. Mahat, Z. Chen, B. Bak-Jensen, and C. L. Bak, "A simple adaptive overcurrent protection of distribution systems with distributed generation," IEEE Transactions on smart grid, vol. 2, no. 3, pp. 428-437, 2011.

[27] W. El-Khattam and T. S. Sidhu, "Resolving the impact of distributed renewable generation on directional overcurrent relay coordination: a case study," IET Renewable power generation, vol. 3, no. 4, pp. 415-425, 2009.

[28] W. K. Najy, H. H. Zeineldin, and W. L. Woon, "Optimal protection coordination for microgrids with grid-connected and islanded capability," IEEE Transactions on industrial electronics, vol. 60, no. 4, pp. 1668-1677, 2012.

[29] S. A. Hosseini, S. H. H. Sadeghi, and A. Nasiri, "Decentralized adaptive protection coordination based on agents social activities for microgrids with topological and operational uncertainties," IEEE Transactions on Industry Applications, vol. 57, no. 1, pp. 702-713, 2020.

[30] Y. Chen, S. Chakraborty, A. Zamzam, and J. Wang, "End-to-end microgrid protection using distributed data-driven methods," Applied Energy, vol. 391, p. 125797, 2025.

[31] P. H. Barra, R. A. Fernandes, and D. V. Coury, "Adaptive hybrid tripping microgrid protection strategy with embedded hardware validation," IEEE Access, 2025.

[32] D. A. Cieslak, M. Moreto, A. E. Lazzaretti, J. R. Junior, F. L. Grando, and T. N. Siemann, "Usage of harmonic synchrophasors for high-impedance fault classification in microgrids," Journal of Control, Automation and Electrical Systems, vol. 35, no. 3, pp. 485-498, 2024.

[33] Digital Techniques, nol. 2, no. 6, pp. 471-482, Nov. 2008, doi: 10.1049/iet-cdt:20070111.

[34] M. Rashedi, A. Khademzadeh, A. Reza, "Elixir: A new band width constrained mapping for Networks-on-chip", IEICE Electronics Express, vol. 7, no. 2, pp. 73-79, Jan. 2010, doi: 10.1587/elex.7.73.

[35] Y. Xie. Y. Liu, "A research on NOC mapping with quantum ant colony algorithm", Proceeding of the IEEE/WiSPNET, pp. 874-877, Chennai, India, March 2017, doi: 10.1109/WiSPNET.2017.8299886.

[36] P. Kaur, S.H. Mehta, "Resource provisioning and work flow scheduling in clouds using augmented shuffled frog leaping algorithm", Journal of Parallel and Distributed Computing, vol. 101, no. 4, pp. 41-50, March 2017, doi: 10.1016/j.jpdc.2016.11.003.

[37] P. Sahu, P. Venkatesh, S. Gollapalli, S. Chattopadhyay, "Application mapping onto mesh structured network-on-chip using particle swarm optimization", Proceeding of the IEEE/ISVLSI, pp. 335-336, Chennai, India, July 2011, doi: 10.1109/ISVLSI.2011.21.

[38] M. Keley, A. Khademzadeh, M. Hosseinzadeh, "Efficient mapping algorithm on mesh-based NoCs in terms of cellular learning automata", International Arab Journal of Information Technology, vol. 16, no. 2, pp. 312-322, March 2019.

[39] B. Broumand, E. Yaghoubi, B. Barekatain, "An enhanced cost-aware mapping algorithm based on improved shuffled frog leaping in network on chip", The Journal of Supercomputing, vol. 77, pp. 498-522, Jan. 2021, doi: 10.1007/s11227-020-03271-5.

[40] P.M. Kalahroudi, E. Yaghoubi, B. Barekatain, "IAM: an improved mapping on a 2-Dnetwork on chip to reduce communicationcost and energy consumption", Photonic Network Communications, vol. 41, pp. 78-99, Feb. 2021, doi: 10.1007/s11107-020-00911-x, 2020.

[41] T. Maqsood, K. Bilal, S. Madani, "Congestion-aware core mapping for Network-on-Chip based systems using betweenness centrality", Future Generation Computer Systems, vol. 82, no. 5, pp. 459-471, May 2018, doi: 10.1016/j.future.2016.12.031.